Current Biology, Vol. 13, 1506–1511, September 2, 2003, ©2003 Elsevier Science Ltd. All rights reserved. DOI 10.1016/S0960-9822(03)00597-9

Caenorhabditis elegans TAC-1 and ZYG-9 Form a Complex that Is Essential for Long Astral and Spindle Microtubules

Martin Srayko, Sophie Quintin, Anne Schwager, and Anthony A. Hyman*
Max-Planck-Institute of Molecular Cell Biology and Genetics
Pfotenhauerstrasse 108
D-01307 Dresden
Germany

Summary

TACC (transforming acidic coiled-coil) proteins were first identified by their ability to transform cell lines [1], and links between human cancer and the overexpression of TACC proteins highlight the importance of understanding the biological function of this family of proteins [2]. Herein, we describe the characterization of a new member of the TACC family of proteins in *Caenorhabditis elegans*, TAC-1. In other systems, TACC proteins associate with the XMAP215 family of microtubule-stabilizing proteins; however, it is unclear whether TACC proteins have microtubule-based functions distinct from XMAP215. We depleted both the XMAP215 ortholog ZYG-9 and TAC-1 via dsRNA-mediated interference (RNAi). We found that *tac-1(RNAi)* resulted in microtubule-based defects that were very similar to *zyg-9(RNAi).* Furthermore, TAC-1 and ZYG-9 are required for long astral microtubules in general and long spindle microtubules during spindle assembly. Loss of either protein did not affect the α-tubulin immunofluorescence intensity near centrosomes; this finding suggests that microtubule nucleation was not compromised. Both proteins localize to centrosomes and the kinetochore/microtubule region of chromosomes in metaphase and early anaphase. Furthermore, we found that ZYG-9 and TAC-1 physically interact in vivo, and this interaction is important for the efficient localization of the ZYG-9/TAC-1 complex to centrosomes.

Results and Discussion

The XMAP215/ch-TOG/Msps family of microtubule-associated proteins binds directly to microtubules (MTs) and promotes MT growth primarily by modulating their dynamic instability [3–7]. The *C. elegans* XMAP215 ortholog ZYG-9 is required for the organization of the meiotic spindle and the formation of long astral microtubules during pronuclear migration and subsequent mitosis [8]. The *Drosophila* ortholog Minispindles (Msps) is also required for MT-based processes, such as the formation and function of the mitotic spindle [9]. Msps was found to physically interact with the *Drosophila* transforming acidic coiled-coil family member D-TACC; moreover, loss of D-TACC function via mutation or antibody injection results in short MTs and spindle defects resembling those in *msps* mutants [10–12].

We identified a homolog of D-TACC in *C. elegans* by conducting BLAST searches with the relatively conserved C-terminal TACC domain of *Drosophila* D-TACC [13, 14] (Figure S1 in the Supplemental Data available with this article online). One predicted *C. elegans* protein encoded by Y54E2A.3 [15] was identified as the closest match. Most TACC protein family members are over 800 amino acids long [14], whereas the Y54E2A.3 protein is only 260 amino acids in length. Furthermore, a predicted *C. briggsae* ortholog CBP15006 is similar in length [16], suggesting that the small size of nematode TACC proteins is a conserved feature. We conclude that the Y54E2A.3 protein represents a novel member of this family and encodes a small coiled-coil protein [17] similar to the C-terminal TACC domain. We refer to this gene as *tac-1*.

To investigate the role of TAC-1 in *C. elegans*, we performed RNAi experiments to deplete the protein [18]. Initial examination of the phenotypes with DIC and fluorescence microscopy of a GFP::Histone; GFP::β-tubulin strain showed that *tac-1(RNAi)* resulted in a failure of oocyte meiosis, pronuclear migration, and mitotic spindle positioning of the one-cell embryo (Figure 1A). These phenotypes are consistent with defects in MTs. The extent and range of phenotypes observed were reminiscent of the MT defects observed in *zyg-9* mutant embryos [8]. To test whether loss of TAC-1 or ZYG-9 results in identical MT-based phenotypes, we focused on the following issues. First, we directly measured astral MT lengths by using indirect immunofluorescence of α-tubulin. MTs that terminate close to the centrosome are difficult to resolve due to the high density of all MTs extending out from the centrosome. Therefore, we identified only the longest MTs and traced their paths back to the centrosome (Figure S2 in the Supplemental Data). Using this method, we determined the average maximal astral MT length in wild-type metaphase to be 11.3 μm, but only 6.3 μm in *zyg-9(RNAi)* and 6.2 μm in *tac-1(RNAi)* ($n = 80$ MTs, from ten MTs per centrosome for each experiment; Figure 1B). Second, we plotted the distance between centrosomes during pronuclear migration of the first prophase (the time when duplicated centrosomes begin to separate) until anaphase onset (Figure 1C). We found that the centrosomes separated around the male pronucleus in both *tac-1(RNAi)* and *zyg-9(RNAi)* (Figure 2B). Therefore, MTs are long enough for maximal separation of centrosomes around the pronuclear sphere. After nuclear envelope breakdown, the first mitotic spindle was smaller (~12.5 μm pole-pole distance in wild-type versus ~8.5 μm in both *zyg-9(RNAi)* and *tac-1(RNAi)*) (Figure 1C). These data indicate that both spindle and astral MTs are shortened to a similar extent by loss of either TAC-1 or ZYG-9. This also supports the idea that spindle length is determined, at least in part, by the dynamic properties of MTs [19]. Finally, we assessed the effect of TAC-1 or ZYG-9 depletion on MT nucleation by measuring the tubulin levels near the centrosome via indirect immunoflu-

*Correspondence: hyman@mpi-cbg.de

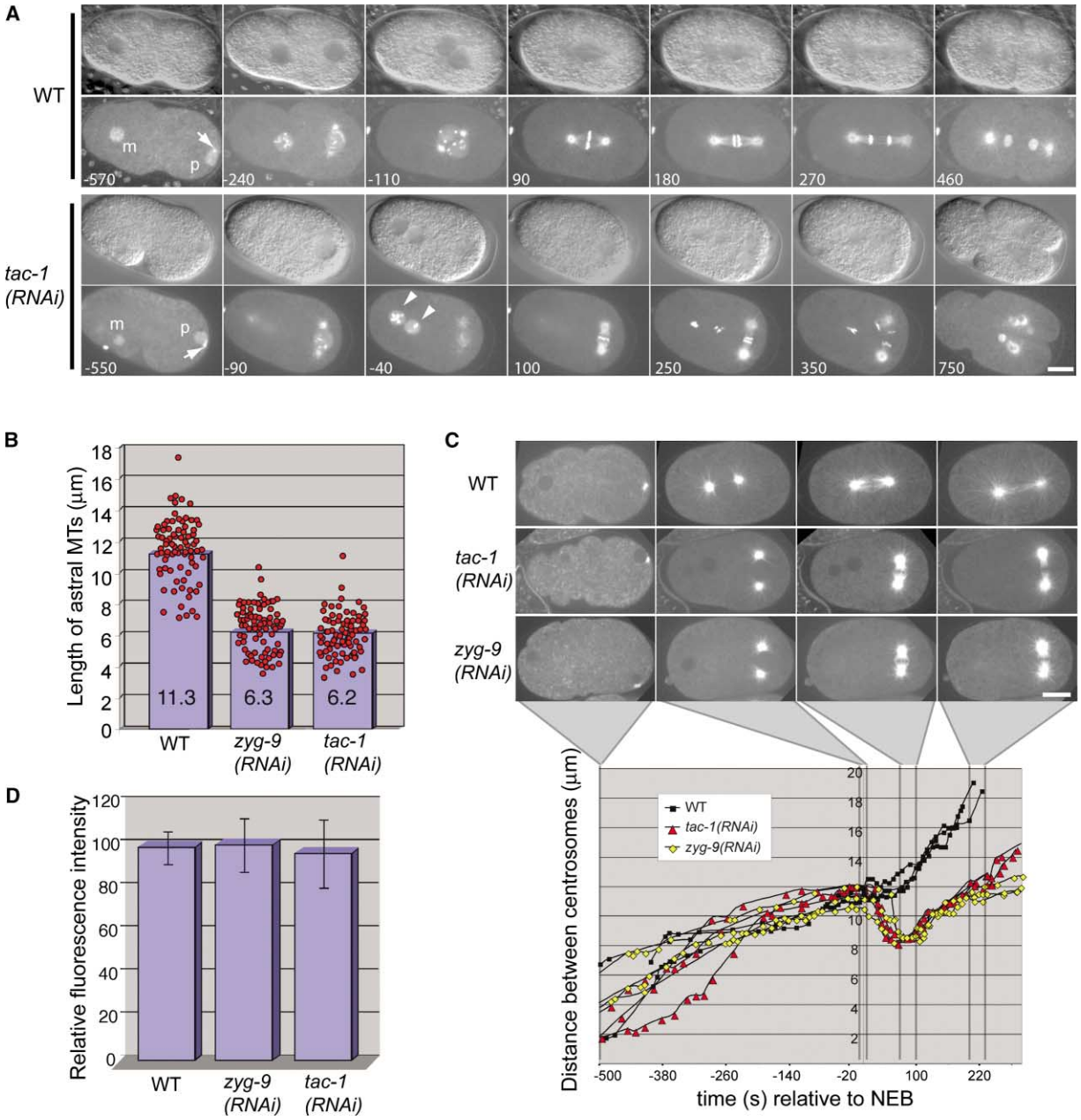

Figure 1. Astral and Spindle MTs Are Shortened in Both *zyg-9(RNAi)* and *tac-1(RNAi)*

(A) DIC and fluorescence images of a wild-type (WT) and *tac-1(RNAi)* embryo from shortly after the completion of female meiosis to the first mitotic telophase are shown (left is oriented toward the anterior). The embryos express both GFP::Histone (chromatin) and GFP::β-tubulin (MTs). Time (s) is relative to nuclear envelope breakdown (NEB). The arrows show centrosomes prior to separation around the paternal pronucleus (p). Multiple maternal nuclei in *tac-1(RNAi)* (arrowheads) indicate failure to efficiently extrude meiotic chromosomes. The maternal nuclei in *tac-1(RNAi)* embryos do not meet with the paternal pronucleus, so the resulting mitotic spindle involves only the paternal chromosomes (at time = 100 s). After NEB, maternal DNA becomes captured by MTs emanating from the centrosomes (e.g., at 350 s). Cytokinesis bisects the spindle; in *tac-1(RNAi)*, ectopic furrows also ingress from the anterior (see the last panel). The scale bar represents 10 μm.

(B) MTs were visualized by indirect immunofluorescence with anti-α-tubulin antibodies. A plot of 80 of the longest MTs from WT, *zyg-9(RNAi)*, and *tac-1(RNAi)* is shown (10 MTs per centrosome, from 4 one-cell embryos in metaphase or early anaphase).

(C) The distance between centrosomes in the one-cell embryo is plotted against time (s) for three embryos of each class. Time is relative to NEB. Representative images from a GFP::β-tubulin strain are shown for four time points.

(D) The relative intensity of anti-α-tubulin near the centrosomes (within a 2.73 μm radius) is presented as an average. Embryos at metaphase/early anaphase were used (n = 30 centrosomes for WT, n = 10 for *zyg-9(RNAi)*, and n = 10 for *tac-1(RNAi)*). SEM is shown (confidence interval = 0.95).

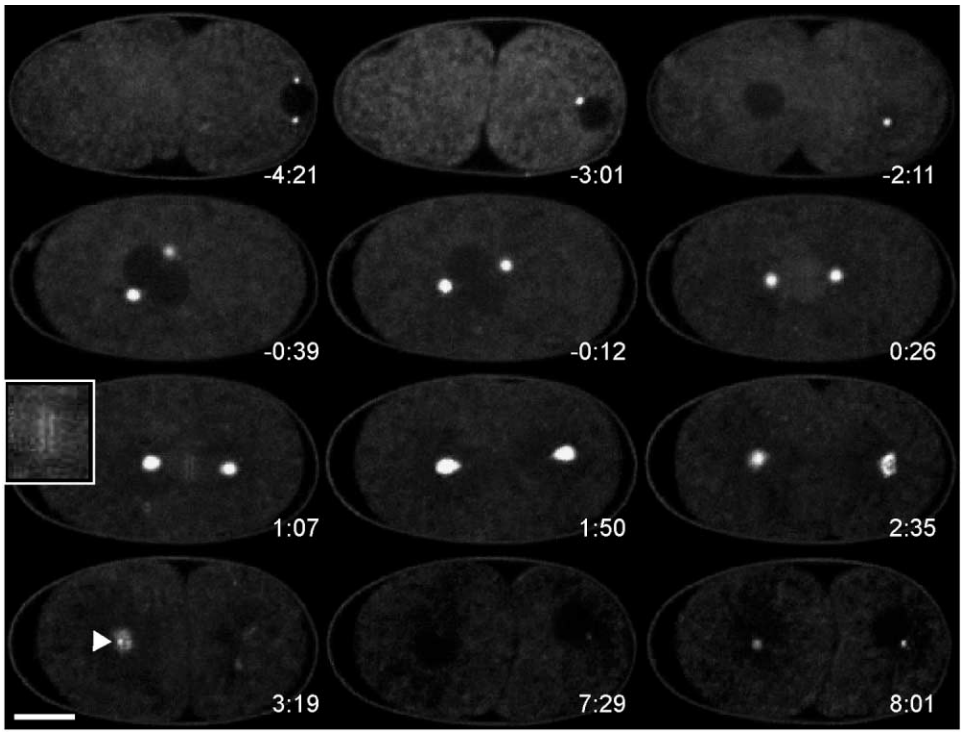

Figure 2. GFP::TAC-1 Locates to Centrosomes and Is Detected at the Kinetochore/MT Interface during Metaphase-Early Anaphase

A time-lapse recording of a GFP::TAC-1 expressing embryo is shown. Time is relative to NEB; left is oriented toward the anterior. TAC-1 is first visible after centrosome separation (in some panels, only one centrosome is in the focal plane). In metaphase and early anaphase, we detect GFP::TAC-1 in the kinetochore/microtubule interface region (inset). A weak signal is also present on spindle microtubules. At the end of cytokinesis, a small dot of GFP fluorescence associated with the disintegrating centrosome is visible (arrowhead), but this signal eventually dissipates (e.g., at time 7:29). The scale bar represents 10 μm. This figure is available as Movie 1 in the Supplemental Data.

orescence. We found that the levels of α-tubulin (Figure 1D) as well as γ- and β-tubulin (Figure S3 in the Supplemental Data) within a 3 μm radius of the centrosome were not significantly different from wild-type. Therefore, the amount of MTs near the centrosome is not dramatically affected by the loss of either TAC-1 or ZYG-9, unlike γ-tubulin for instance, which has a profound effect on the ability of centrosomes to nucleate MTs in *C. elegans* [20]. From these data, we conclude that the broad range of MT-based phenotypes that occurs in both *tac-1(RNAi)* and *zyg-9(RNAi)* is best explained by the shortening of all MTs emanating from the centrosome as a consequence of reduced MT stability. The MT shortening is likely not due to problems with nucleating MTs since we did not detect any decrease in the amount of MTs near the centrosomes in either *tac-1(RNAi)* or *zyg-9(RNAi)*. This contrasts with recent evidence implicating XMAP215 in the nucleation of MTs in *Xenopus* oocyte extracts [21], and these data may reflect divergence of the specific activity of the XMAP215 family members. While our data does agree with the MT-stabilizing behavior of XMAP215 and Msps, clearly not all family members share this activity. For instance, the distantly related yeast family member Stu2p has been shown to exhibit MT-destabilizing activity in vitro [22]. Also, XMAP215 itself does induce depolymerization of GMPCPP-stabilized MTs [23]. In order to explain this apparent contradiction, it has been proposed that XMAP215 proteins may alter the pause state of MTs, with subsequent catastrophe or further growth of the MT depending on other conditions, such as the availability of free tubulin [23]. Therefore, the cytoplasmic environment may also determine the effect that XMAP215 members have on MT behavior.

If TAC-1 is required for the function of the XMAP215-like protein ZYG-9, then we expect the two proteins to be at the same intracellular location. In order to assess the location of the TAC-1 protein, we constructed a GFP::TAC-1 worm strain. Using Nipkow spinning disk confocal microscopy, we observed GFP fluorescence at the centrosomes early in pronuclear migration, although we could only detect a signal after separation of the centrosomes (Figure 2). This is consistent with our results above; neither TAC-1 nor ZYG-9 are required for centrosome separation. The GFP signal at the centrosomes increased in intensity throughout the cell cycle, as has been reported for ZYG-9 [8, 24]. At metaphase and early anaphase, we also observed fluorescence at the MT/kinetochore interface (Figure 2, inset). Anti-TAC-1 antibodies confirmed all patterns observed with the GFP strain (Figure 3 and data not shown). However, the kinetochore staining was not always visible in fixed samples, perhaps due to epitope sensitivity to fixation in this region. Together, the location patterns for TAC-1 were highly similar to those previously reported for ZYG-9 based on immunostaining [8].

Immunolocalization studies in *Drosophila* showed that efficient localization of Msps to centrosomes relies on

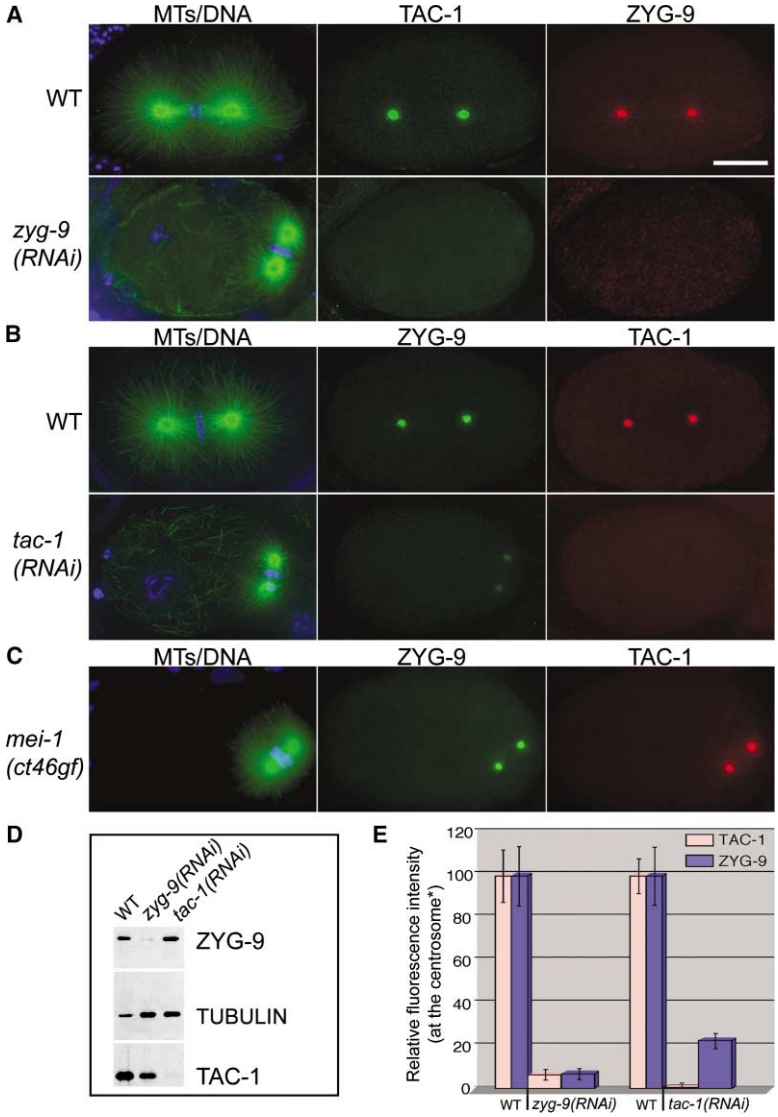

Figure 3. ZYG-9 Is Required for Detection of TAC-1 at Centrosomes, but Some ZYG-9 Can Locate to Centrosomes in the Absence of TAC-1

Images of embryos fixed and immunostained with anti-α-tubulin (green), anti-TAC-1, or anti-ZYG-9 antibodies are shown. DNA (blue) is visualized with Hoechst.

(A) In *zyg-9(RNAi)* embryos, both ZYG-9 and TAC-1 protein levels are greatly reduced at the centrosomes.

(B) *tac-1(RNAi)* embryos contain no detectable TAC-1; however, we detect a fraction of ZYG-9 at the centrosome.

(C) Both ZYG-9 and TAC-1 are present at centrosomes in *mei-1(ct46gf)* mutant embryos, which exhibit a similar microtubule-shortening phenotype, albeit due to ectopic microtubule severing.

(D) A Western blot probed with anti-ZYG-9, anti-TAC-1, and anti-α-tubulin antibodies (see the Experimental Procedures).

(E) A comparison of the amount of fluorescence detected at metaphase (or early anaphase) for ≥10 centrosomes from one-cell embryos. All values are relative to corresponding WT controls for each experiment. For the *zyg-9(RNAi)*, we chose embryos with 5%–10% ZYG-9 (average = 7.6%) at the centrosome; TAC-1 levels were an average of 7.1%. In examples in which ZYG-9 was less than 5%, TAC-1 was undetectable (e.g., [B]). For *tac-1(RNAi)*, we chose six embryos that had <1% TAC-1; in these embryos, we observed an average of 22.1% ZYG-9. The scale bars indicate SEM (confidence interval = 0.95).

D-TACC and vice versa [11, 12]. To test whether TAC-1 is required for the location of ZYG-9 and vice versa, we immunostained embryos after RNAi treatment. When ZYG-9 was depleted from embryos, we consistently observed a correlated decrease in TAC-1 at the centrosome (Figures 3A and 3E). In embryos having less than 5% ZYG-9 remaining at centrosomes, we observed less than 0.5% TAC-1 (n = 3; data not shown). For embryos having more than 5% ZYG-9 (average of 7.6%), TAC-1 was detected at the same or lower levels (average of 7.1%; n = 10 centrosomes; Figure 4E). This result suggests that TAC-1 directly depends on ZYG-9 for its centrosomal location. However, Western blot analysis showed that in *zyg-9(RNAi)* embryos, the TAC-1 protein levels are also reduced (approximately 1/8 of wild-type levels; see the Experimental Procedures). Therefore, we are unable to make a strong statement regarding the ability of TAC-1 to locate to centrosomes in the absence of ZYG-9. By comparison, *Drosophila msps* mutants seem to have a less pronounced effect on D-TACC localization; a small amount of Msps protein is still present in *msps* embryos, which may account for the difference [11, 12].

In contrast to the above experiment, we always observed a significant amount of ZYG-9 at the centrosomes when TAC-1 was depleted (Figure 3B). Quantification of this signal showed that an average of 22.1% of ZYG-9 was still present at centrosomes having less than 1% TAC-1 (n = 10 centrosomes; Figure 3E). Therefore, some ZYG-9 is capable of locating to the centrosomes in the absence of TAC-1. Western blot analysis showed that in *tac-1(RNAi)* embryos, the ZYG-9 protein is still present at approximately 1/2 of wild-type levels (Figure 3D; see the Experimental Procedures). Therefore, differential stabilities of ZYG-9 and TAC-1 may also contribute to the observed differences in the immunofluorescence experiments described above. In a similar set of experiments by Le Bot et al. [25], the authors found that ZYG-9 is completely dependant on TAC-1 for centrosomal location. However, protein stability may be greatly affected by different RNAi conditions, for example, incubation time and temperature after RNAi in-

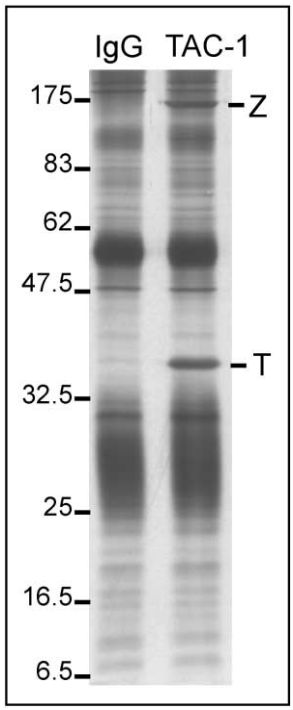

Figure 4. ZYG-9 Coimmunoprecipitates with TAC-1

Protein-A bound IgG or TAC-1 antibodies were incubated with gravid adult worm lysate and washed, and the eluted proteins were separated via SDS-PAGE. The gel was silver stained with slight overdeveloping to show any potential interacting partners. MALDI peptide mapping identified the two prominent bands as TAC-1 (T) and ZYG-9 (Z). The positions of size standards (with their M.W. given in kDa; New England Biolabs) are shown.

jection (see the Experimental Procedures). Alternatively, variation in the sensitivity of our respective antibodies could account for the differences observed.

In both *tac-1(RNAi)* and *zyg-9(RNAi)*, the MTs are shorter during mitosis. To control for the possibility that the staining patterns observed were due to the shortening of MTs and not to the absence of either TAC-1 or ZYG-9 per se, we performed a similar experiment with the mutation *mei-1(ct46gf)*. *mei-1(ct46gf)* results in defects that closely resemble the *zyg-9* and *tac-1* phenotypes reported here; however, the basis for the MT shortening is due to ectopic mitotic activity of the katanin MT-severing homolog MEI-1/MEI-2 [26]. In these embryos, we observed both TAC-1 and ZYG-9 at the centrosome (Figure 3C). Therefore, shortened MTs that cause a similar spindle mispositioning phenotype do not decrease the amount of TAC-1 or ZYG-9 at the centrosome.

ZYG-9 and TAC-1 exhibit the same pattern of intracellular location, and both loss-of-function phenotypes are identical based on assays performed in this study. Furthermore, the RNAi experiments above suggest interdependency regarding localization and protein stability. Therefore, it is likely that these two proteins physically interact. To test this, we immunoprecipitated TAC-1 from wild-type, gravid adult lysates and looked for any potential interacting proteins. After elution of all proteins bound to anti-TAC-1 protein-A beads, SDS-PAGE and silver staining revealed only two major bands not present in the IgG bead control lane (Figure 4). Both the suspected TAC-1 bait band and the ~160 kDa MW band were excised and sequenced via MALDI peptide mapping (MASS Spectrophotometry Service Facility, Dresden). The large MW band was identified as ZYG-9, and the small MW band was identified as TAC-1. Therefore, we conclude that TAC-1 and ZYG-9 interact in vivo. Despite the small size of this TACC family member, it appears that the ability to interact with its XMAP215 counterpart is conserved. This is consistent with experiments in *Drosophila* that showed that the C-terminal TACC domain (see Figure S1) is sufficient to localize to centrosomes and interact with Msps [10, 12].

Conclusions

Taken together, our results show that ZYG-9 and TAC-1 form a complex that is required for the formation of long microtubules in the early embryo, but our data suggest that this complex is not required for efficient nucleation of microtubules. If this complex is not required for nucleation, why is its predominant location at the centrosome? One possibility is that ZYG-9/TAC-1 binds to and stabilizes the microtubule plus end concomitant with nucleation. While there is no evidence outside of the kinetochore/MT interface for plus end localization of ZYG-9 [8] and TAC-1 (this study), this may be a limitation of the microscopy of *C. elegans*. Indeed, the *S. cerevisiae* XMAP215 homolog Stu2p has been observed at plus ends, both in vivo [27] and in vitro [22]. This would be consistent with the emerging concept that many regulators of microtubule function may load onto spindle poles, as shown for yeast Kar9, for example [28].

Supplemental Data

Supplemental Data including a sequence alignment of TAC-1 with the *Drosophila* D-TACC domain and the human TACC-1 C terminus, the method for MT length measurements, quantification of γ- and β-tubulin levels at the centrosome, a GFP::TAC-1 movie, and Experimental Procedures are available at http://www.current-biology.com/cgi/content/full/13/17/1506/DC1/.

Acknowledgments

We thank Stephan Grill, Kazuhisa Kinoshita, Eric Marois, Tim Nötzel, and Laurence Pelletier for comments on the manuscript, Bianca Habermann for Bioinformatics support, and Anna Shevchenko and Andrej Shevchenko for MASS Spectrophotometry. Some worm strains were received from T. Stiernagle at the *Caenorhabditis* Genetics Center. This work was supported by a Human Frontier Long-Term Fellowship to M.S. and a Marie Curie Individual Fellowship from the European Commission to S.Q.

Received: June 2, 2003
Revised: July 7, 2003
Accepted: July 8, 2003
Published: September 2, 2003

References

1. Still, I.H., Hamilton, M., Vince, P., Wolfman, A., and Cowell, J.K. (1999). Cloning of TACC1, an embryonically expressed, potentially transforming coiled coil containing gene, from the 8p11 breast cancer amplicon. Oncogene *18*, 4032–4038.
2. Raff, J.W. (2002). Centrosomes and cancer: lessons from a TACC. Trends Cell Biol. *12*, 222–225.
3. Gard, D.L., and Kirschner, M.W. (1987). A microtubule-associ-

ated protein from *Xenopus* eggs that specifically promotes assembly at the plus-end. J. Cell Biol. *105*, 2203–2215.
4. Tournebize, R., Popov, A., Kinoshita, K., Ashford, A.J., Rybina, S., Pozniakovsky, A., Mayer, T.U., Walczak, C.E., Karsenti, E., and Hyman, A.A. (2000). Control of microtubule dynamics by the antagonistic activities of XMAP215 and XKCM1 in *Xenopus* egg extracts. Nat. Cell Biol. *2*, 13–19.
5. Vasquez, R.J., Gard, D.L., and Cassimeris, L. (1999). Phosphorylation by CDK1 regulates XMAP215 function in vitro. Cell Motil. Cytoskeleton *43*, 310–321.
6. Kinoshita, K., Habermann, B., and Hyman, A.A. (2002). XMAP215: a key component of the dynamic microtubule cytoskeleton. Trends Cell Biol. *12*, 267–273.
7. Ohkura, H., Garcia, M.A., and Toda, T. (2001). Dis1/TOG universal microtubule adaptors - one MAP for all? J. Cell Sci. *114*, 3805–3812.
8. Matthews, L.R., Carter, P., Thierry-Mieg, D., and Kemphues, K. (1998). ZYG-9, a *Caenorhabditis elegans* protein required for microtubule organization and function, is a component of meiotic and mitotic spindle poles. J. Cell Biol. *141*, 1159–1168.
9. Cullen, C.F., Deak, P., Glover, D.M., and Ohkura, H. (1999). *mini spindles*: a gene encoding a conserved microtubule-associated protein required for the integrity of the mitotic spindle in *Drosophila*. J. Cell Biol. *146*, 1005–1018.
10. Gergely, F., Kidd, D., Jeffers, K., Wakefield, J.G., and Raff, J.W. (2000). D-TACC: a novel centrosomal protein required for normal spindle function in the early *Drosophila* embryo. EMBO J. *19*, 241–252.
11. Cullen, C.F., and Ohkura, H. (2001). Msps protein is localized to acentrosomal poles to ensure bipolarity of *Drosophila* meiotic spindles. Nat. Cell Biol. *3*, 637–642.
12. Lee, M.J., Gergely, F., Jeffers, K., Peak-Chew, S.Y., and Raff, J.W. (2001). Msps/XMAP215 interacts with the centrosomal protein D-TACC to regulate microtubule behaviour. Nat. Cell Biol. *3*, 643–649.
13. Gergely, F., Karlsson, C., Still, I., Cowell, J., Kilmartin, J., and Raff, J.W. (2000). The TACC domain identifies a family of centrosomal proteins that can interact with microtubules. Proc. Natl. Acad. Sci. USA *97*, 14352–14357.
14. Gergely, F. (2002). Centrosomal TACCtics. Bioessays *24*, 915–925.
15. Stein, L., Sternberg, P., Durbin, R., Thierry-Mieg, J., and Spieth, J. (2001). WormBase: network access to the genome and biology of *Caenorhabditis elegans*. Nucleic Acids Res. *29*, 82–86.
16. Harris, T.W., Lee, R., Schwarz, E., Bradnam, K., Lawson, D., Chen, W., Blasier, D., Kenny, E., Cunningham, F., Kishore, R., et al. (2003). WormBase: a cross-species database for comparative genomics. Nucleic Acids Res. *31*, 133–137.
17. Lupas, A., Van Dyke, M., and Stock, J. (1991). Predicting coiled coils from protein sequences. Science *252*, 1162–1164.
18. Fire, A., Xu, S., Montgomery, M.K., Kostas, S.A., Driver, S.E., and Mello, C.C. (1998). Potent and specific genetic interference by double-stranded RNA in *Caenorhabditis elegans*. Nature *391*, 806–811.
19. Andersen, S.S. (2000). Spindle assembly and the art of regulating microtubule dynamics by MAPs and Stathmin/Op18. Trends Cell Biol. *10*, 261–267.
20. Hannak, E., Oegema, K., Kirkham, M., Gonczy, P., Habermann, B., and Hyman, A.A. (2002). The kinetically dominant assembly pathway for centrosomal asters in *Caenorhabditis elegans* is gamma-tubulin dependent. J. Cell Biol. *157*, 591–602.
21. Popov, A.V., Severin, F., and Karsenti, E. (2002). XMAP215 is required for the microtubule-nucleating activity of centrosomes. Curr. Biol. *12*, 1326–1330.
22. Van Breugel, M., Drechsel, D., and Hyman, A. (2003). Stu2p, the budding yeast member of the conserved Dis1/XMAP215 family of microtubule-associated proteins is a plus end-binding microtubule destabilizer. J. Cell Biol. *161*, 359–369.
23. Shirasu-Hiza, M., Coughlin, P., and Mitchison, T. (2003). Identification of XMAP215 as a microtubule-destabilizing factor in *Xenopus* egg extract by biochemical purification. J. Cell Biol. *161*, 349–358.
24. Hannak, E., Kirkham, M., Hyman, A.A., and Oegema, K. (2001). Aurora-A kinase is required for centrosome maturation in *Caenorhabditis elegans*. J. Cell Biol. *155*, 1109–1116.
25. Le Bot, N., Tsai, M.-C., Andrews, R.K., and Ahringer, J. (2003). TAC-1, a regulator of microtubule length in the *C. elegans* embryo. Curr. Biol. *13*, 1499–1505.
26. Srayko, M., Buster, D.W., Bazirgan, O.A., McNally, F.J., and Mains, P.E. (2000). MEI-1/MEI-2 katanin-like microtubule severing activity is required for *Caenorhabditis elegans* meiosis. Genes Dev. *14*, 1072–1084.
27. He, X., Rines, D.R., Espelin, C.W., and Sorger, P.K. (2001). Molecular analysis of kinetochore-microtubule attachment in budding yeast. Cell *106*, 195–206.
28. Liakopoulos, D., Kusch, J., Grava, S., Vogel, J., and Barral, Y. (2003). Asymmetric loading of Kar9 onto spindle poles and microtubules ensures proper spindle alignment. Cell *112*, 561–574.